ELSEVIER

Biochimica et Biophysica Acta 1556 (2002) 29–40

BIOCHIMICA ET BIOPHYSICA ACTA
BBA

www.bba-direct.com

The Lhca antenna complexes of higher plants photosystem I☆

Roberta Croce[a,1], Tomas Morosinotto[a], Simona Castelletti[a,b], Jacques Breton[c], Roberto Bassi[a,*]

[a] *Dipartimento Scientifico e Tecnologico, Università di Verona, Strada Le Grazie, 15-37234 Verona, Italy*
[b] *Departement de Biologie Cellulaire et Moleculaire, CEA-Saclay, France*
[c] *Service de Bioénergétique, Bât. 532 CEA-Saclay, 91191, Gif-sur-Yvette, France*

Received 15 April 2002; received in revised form 19 June 2002; accepted 26 July 2002

Abstract

The Lhca antenna complexes of photosystem I (PSI) have been characterized by comparison of native and recombinant preparations. Eight Lhca polypeptides have been found to be all organized as dimers in the PSI–LHCI complex. The red emission fluorescence is associated not only with Lhca1–4 heterodimer, but also with dimers containing Lhca2 and/or Lhca3 complexes. Reconstitution of Lhca1 and Lhca4 monomers as well as of the Lhca1–4 dimer in vitro was obtained. The biochemical and spectroscopic features of these three complexes are reported. The monomers Lhca1 and Lhca4 bind 10 Chls each, while the Chl *a*/*b* ratio is lower in Lhca4 as compared to Lhca1. Three carotenoid binding sites have been found in Lhca1, while only two are present in Lhca4. Both complexes contain lutein and violaxanthin while β-carotene is selectively bound to the Lhca1–4 dimer in substoichiometric amounts upon dimerization. Spectral analysis revealed the presence of low energy absorption forms in Lhca1 previously thought to be exclusively associated with Lhca4. It is shown that the process of dimerization changes the spectroscopic properties of some chromophores and increases the amplitude of the red absorption tail of the complexes. The origin of these spectroscopic features is discussed.

Keywords: Photosynthesis; Chlorophyll-protein; Recombinant Lhc protein

1. Introduction

Photosystem I (PSI), a multi-subunit complex located in the stroma lamellae of thylakoid membranes, is a plastocyanine/ferredoxin oxido-reductase. The complex from higher plants can be divided in two moieties: (i) the core complex, composed of 14 subunits, which contains the primary donor P700 and all the cofactors of the electron transport chain as well as about 100 Chl *a* and 20 β-carotene molecules with antenna function [1–3]; and (ii) the external antenna composed of four polypeptides, belonging to the Lhc family and named Lhca1–4, with molecular weight between 21 and 24 kDa [3,4]. These polypeptides bind to one side of the core complex [5] by interactions with PsaF, PsaG, and PsaK subunits [6,7]. LHCI proteins coordinate Chl *a*, Chl *b*, lutein, violaxanthin, and small amount of β-carotene [8,9]. On the basis of the high sequence homology of these polypeptides with the major LHCII antenna complex, it has been proposed that Lhca proteins share a high degree of structural similarity with the LHCII proteins [10]. Currently, little information is available on individual Lhca, mainly due to difficulties in purification. Most of the data on Lhca complexes have been obtained by studying a fraction containing all of the complexes [11,12] or two sub fractions, namely LHCI-730 and LHCI-680, which were suggested to consist of dimeric Lhca1–4 and monomeric Lhca2-(3) complexes, respectively [13,14]. More recently, Lhca1 and Lhca4 were reconstituted in vitro in both monomeric and heterodimeric forms [15], allowing time-resolved studies on homogeneous preparations [16,17].

The absorption spectrum of the PSI–LHCI supramolecular complex is characterized by the presence of chlorophyll forms that absorb at lower energy than the reaction center. It has been shown that at RT more than 80% of the energy is present in these forms and has to be transferred energetically uphill to be used for photosynthesis [18]. The "red forms" have been extensively analyzed both in bacteria and higher

☆ A part of the experiments included in this paper has been previously published in the Proceedings of the XI International Conference on Photosynthesis (ed. G. Garab).

* Corresponding author. Tel.: +39-45-8027916; fax: +39-45-8027929
E-mail address: bassi@sci.univr.it (R. Bassi).
[1] Present address: Istituto di Biofisica, CNR Milano, Via Celoria 26, 20133, Milano, Italy.

0005-2728/02/$ - see front matter © 2002 Elsevier Science B.V. All rights reserved.
PII: S0005-2728(02)00304-3

plants. However, information about their function and localization are still controversial (for a review see Ref. [19] and references therein). In higher plants it has been proposed that most of the red forms are associated with the external antenna, particularly Lhca4 [15,20,21]. It has also been suggested that Lhca2 and Lhca3 are responsible for the 680-nm emission and therefore do not bind "red Chls". More recently, the analysis of a fraction containing all of the Lhca proteins indicated that some of the red forms can also be associated with these Lhca2 and/or Lhca3 [11]. Analysis of anti-sense plants depleted on these proteins supports this suggestion [22].

In this work, we analyzed LHCI complexes either purified from higher plants or reconstituted in vitro, in order to study the biochemical and spectroscopic properties of Lhca proteins.

2. Material and methods

2.1. Purification and analysis of the native complexes

Native complexes were purified from *Zea mays* and *Arabidopsis thaliana* as already reported [23]. The sample buffer was 10 mM tricine pH 7.8, 0.3 M sucrose, and 0.03% β-DM, and samples were frozen until use. Size-exclusion chromatography was performed using a Bio Select, SEC-125-5 (300 × 7.8 mm) Bio-Rad column. The elution buffer was 50 mM $NaHPO_3$, 150 mM NaCl, and 0.025% DM, and the flow rate was 0.8 ml/min.

Cross-linking experiments were performed using different concentrations of gluteraldehyde (0.5%, 1%, 2%). The sample concentration was 10 μg/ml of Chl. The solutions were left in ice for 20 min and then blocked with 1/40 vol of $NaBH_4$ (in 2 M NaOH).

2.2. Electrophoresis and nondenaturing iso-electro-focalization

SDS-PAGE tris–sulfate was performed as reported in Ref. [24]. Nondenaturing electrophoresis was performed as in Ref. [25], but using 0.05% of SDS in the superior buffer, in the dark at 4 °C.

Nondenaturing IEF was performed as reported in Ref. [26]. Green fractions were identified in the 3.9–4.55 pH range.

2.3. DNA constructions

Plasmids were constructed using standard molecular cloning procedures [27]. Bacterial hosts were *Escherichia coli* DH5α strain [28] and SG13009 strain [29]. cDNA of Lhca1 and Lhca4 from *A. thaliana* were supplied by Arabidopsis Biological Resource Center (ABRC) at the Ohio State University. The sequences codifying for the mature proteins were subcloned in pQE 50 by Qiagen.

2.4. Isolation of overexpressed Lhca apoproteins from bacteria

Lhca apoproteins were isolated from the SG13009 strain transformed with Lhca1 and Lhca4 constructs following a protocol previously described [30,31].

2.5. Reconstitution and purification of Lhca–pigment complexes

These procedures were performed as described in Ref. [32] with the following modifications: in the reconstitution mix we always add 420 μg of apoprotein, 240 μg of chlorophyll and 60 μg of carotenoid. The Chl *a*/*b* ratio in the pigment mixture was 4 for all reconstitutions and the carotenoid composition in the mixture was reflecting the composition in the thylakoid membrane (lutein, neoxanthin, violaxanthin, and b-carotene, respectively 4:3:2:1). The pigments used were purified from spinach thylakoids.

2.6. Pigment analysis and pigment/protein stoichiometry

The pigment complement of the holoprotein was analyzed by HPLC [33] and fitting of the acetone extract with the spectra of the individual pigments [34]. The protein was quantified by ninhydrin method [35] and by SDS-PAGE analysis [36].

2.7. Spectroscopy

The absorption spectra at RT were recorded by SLM-Aminco DK2000 spectrophotometer, in 10 mM Hepes pH 7.5, 20% glycerol, and 0.06% β-DM; 0.4-nm step was used. The fluorescence emission spectra were measured on Jasco FP-777 fluorimeter at RT and 77 K and corrected for the instrumental response. The samples were excited at 440, 475, and 500 nm. The band widths were 5 nm in excitation and 3 nm in emission. For the excitation spectra the emission were recorded at 685 and 720 nm. All fluorescence spectra were measured at 0.02 OD at the maximum of Q_y transition.

LD spectra were obtained as described in Refs. [37,38] using samples oriented by the polyacrylamide gel squeezing technique.

The CD spectra were measured at 10 °C on a Jasco 600 spectropolarimeter. The samples were in the same solution described for the absorption. All the spectra presented were normalized to the same polypeptide concentration, based on the Chl binding stoichiometry [39].

Denaturation temperature measurements were performed by following the decay of the CD signal at 459 nm when increasing the temperature from 20 to 80 °C with a time slope of 1 °C per min and a resolution of 0.2 °C. The thermal stability of the protein was determined by finding the $t_{1/2}$ of the signal decay.

2.8. Analysis of the Q_y region of the spectra

Spectral forms of Chlorophyll *a* and *b* in pigment–protein complexes between 630 and 720 nm was determined by Cinque et al. [40]. These forms were utilized for a fitting of the absorption spectrum of Lhca1 in this interval [34].

3. Results

Both PSI and PSII have an antenna moiety constituted by Lhc polypeptides binding Chl *a*, Chl *b*, and xanthophylls. While the components of the PSII antenna have been characterized in detail leading to an overall knowledge of several aspects of the PSII–LHCII organization including supramolecular organization of subunits [41,42], stoichiometry of protein, pigment components [43] and distribution of different pigment species into individual binding sites within Lhc gene products [44,45], the knowledge of PSI antenna system components is still insufficient due to the difficulty in the purification of individual Lhca gene products. In this study we have integrated the study of native complexes isolated from thylakoids with that of recombinant Lhca1 and -4 pigment proteins and obtained an improved picture of PSI–LHCI organization.

3.1. Native LHCI

LHCI complexes were purified from *A. thaliana* and *Z. mays* as reported previously [23]. Fig. 1A shows the SDS-PAGE analysis of the LHCI fraction as compared to that of the PSI–LHCI original preparation, while Fig. 1B shows the densitometric analysis. The polypeptide patterns of the LHCI and PSI core were complementary in yielding the PSI–LHCI pattern in both composition and relative amounts, thus ensuring that no polypeptides have been lost during purification. This was further confirmed by immunoblot analysis with anti-Lhca1–4 antibodies (not shown).

The pigment content of the LHCI fractions was analyzed by HPLC and fitting of the spectrum of the acetone extract was performed with the spectra of the individual pigments in this solvent. The data are reported in Table 1. The Chl *a*/*b* ratio of the preparations was 3.8 for *Z. mays* and 3.3 for *A. thaliana*, while the Chl/Car ratio was 4.6 in both cases. Only three carotenoid species were found in the complexes, namely lutein, violaxanthin, and β-carotene. Neoxanthin was not present, in agreement with previous results [9].

The pigment-to-protein stoichiometry was calculated for LHCI from *Z. mays* by independent determination of Chl and protein concentrations. A value of 10 Chls per polypeptide was obtained. Due to the presence of four polypeptides in the preparation, this value represents the average number of Chls bound to Lhca polypeptides. The pigment–protein ratio of LHCI in *A. thaliana* was the same as in *Z. mays*, suggesting that although the relative amount of Chl *a* and *b* can differ between the two species, the overall number of chromophores per polypeptide is conserved.

The aggregation state of Lhca complexes was tested in the *Z. mays* preparation by four different methods: size exclusion chromatography, nondenaturing gel electrophore-

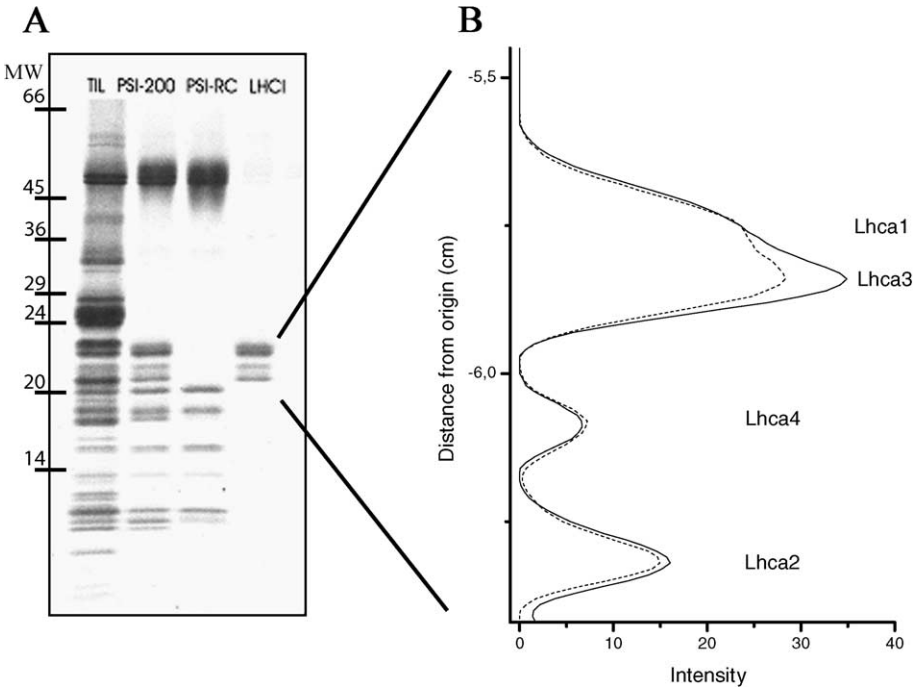

Fig. 1. LHCI purification. (A) SDS-PAGE of the LHCI purification steps: line 1: thylakoids; line 2: PSI-200; line 3: PSI-core; line 4: LHCI. (B) Densitometric analysis of the LHCI region (about 20–24 kDa) of lines 2 (solid) and 4 (dotted). The distance from the origin is measured from the protein gel.

Table 1
Pigment composition of reconstituted complexes

Sample	Chl *a*/*b*	Chl/car	Neo	Viola	Lute	β-Carotene	Denaturation temperature (° C)
nLHCI Zm	3.8 ± 0.2	4.6 ± 0.1	–	0.55	1.2	0.4	nd
nLHCI Ar	3.3 ± 0.1	4.6 ± 0.1	–	0.6	1.1	0.45	57
rLhca1	4.0 ± 0.1	3.3 ± 0.1	0.12	1.05	1.81	–	54
rLhca4	2.3 ± 0.2	4.9 ± 0.2	–	0.5	1.5	–	45
rLhca1–4	3.0 ± 0.2	4.0 ± 0.1	0.08	0.8	1.2	0.4	56

All complexes have been reconstituted with Chl *a*/*b* ratio of 4.0 in the pigment mix and in the presence of the full car complement.

sis, sucrose gradient ultracentrifugation, and cross-linking (Fig. 2A–D). In the first three experiments, LHCII monomers and trimers were used as a standard. In size exclusion chromatography, the retention time of LHCI was intermediate between monomeric and trimeric LHCII (Fig. 2A). The same results were obtained in sucrose gradient ultracentrifugation, where LHCI proteins were found in band 2 (Fig. 2B), with a sedimentation factor value in between the two aggregation states of LHCII. The presence of a band at approximately 44 kDa (Fig. 2D) in the cross-linking experiments confirms that the aggregation state is dimeric. This was also corroborated further by nondenaturing gel electrophoresis (Fig. 2C). In addition, the latter experiment clearly indicates that no monomers were present in the preparation. The same results were obtained for the *Arabidopsis* preparation, where all Lhca complexes were found in a single sucrose gradient band that exhibited the characteristics of the dimer. We can therefore conclude that Lhca proteins are organized as dimers in vivo.

In order to purify different dimers, the LHCI fraction was subjected to nondenaturing IEF followed by sucrose gradient ultracentrifugation. Although it was not possible to

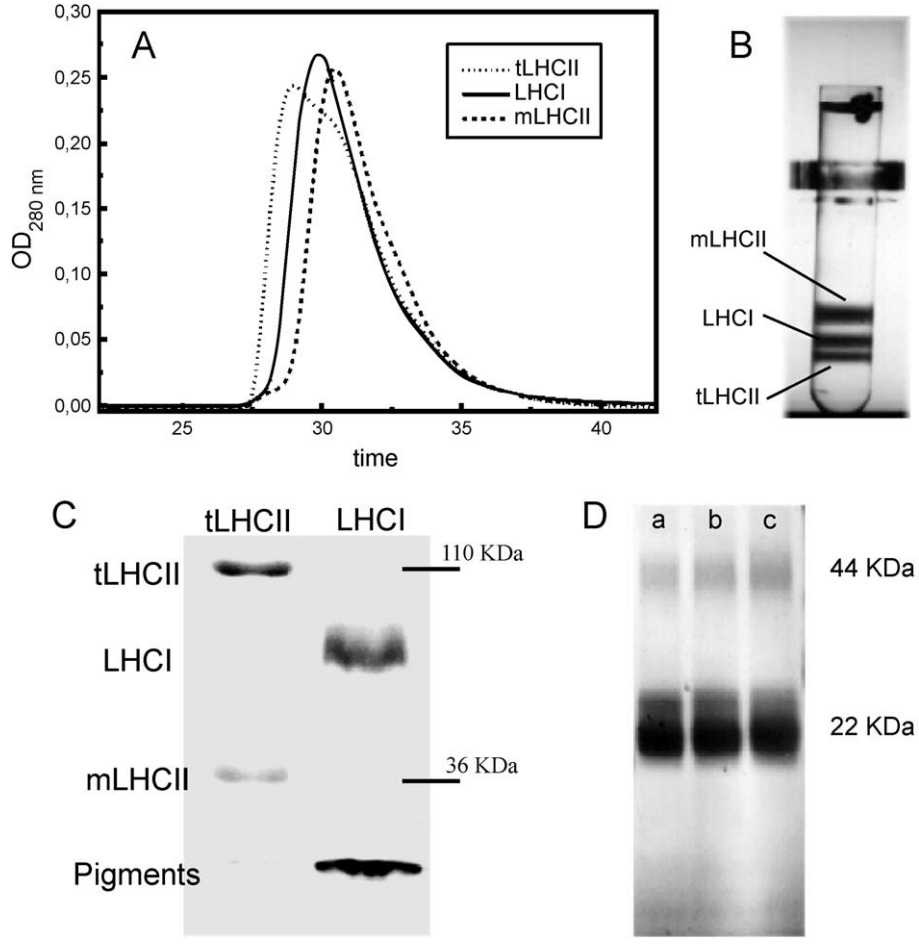

Fig. 2. Determination of the aggregation state of Lhca complexes. (A) Size exclusion chromatography. The retention time of LHCI fraction (solid) is compared with the retention times of LHCII trimers (dotted) and monomers (dashed). (B) Sucrose gradient. The mobility of Lhca complexes is compared with LHCII trimers and monomers. (C) Nondenaturing gel electrophoresis. Line 1: LHCII trimer and monomer; line 2: LHCI fraction. (D) Cross-linking experiments in which LHCI fraction was treated with different amounts of gluteraldehyde: line a, 0.5%; line b, 1%; line c, 2%.

purify the dimers to homogeneity, fractions enriched in individual polypeptides were obtained, as detected by SDS-PAGE (Fig. 3A). In Fig. 3B, the absorption spectra of two fractions, called LHCI-A and LHCI-B, containing 80% of Lhca1/4 and 70% of Lhca2/3, respectively, are shown. The absorption maxima of the two fractions were 680.0 and 681.5 nm, respectively. The red absorption tail is present in both spectra and displays very similar intensity. The fluorescence spectra at RT of the two fractions are reported in Fig. 3C, together with the fluorescence spectrum of the starting material (LHCI). The spectrum maxima are at 685.0 nm and have a broad shoulder at higher wavelengths, typical of PSI antenna complexes [3]. Although LHCI-A (containing Lhca1–4) showed enhanced red emission as compared to the starting material, the LHCI-B spectrum also has a substantial contribution from the red-shifted emission band.

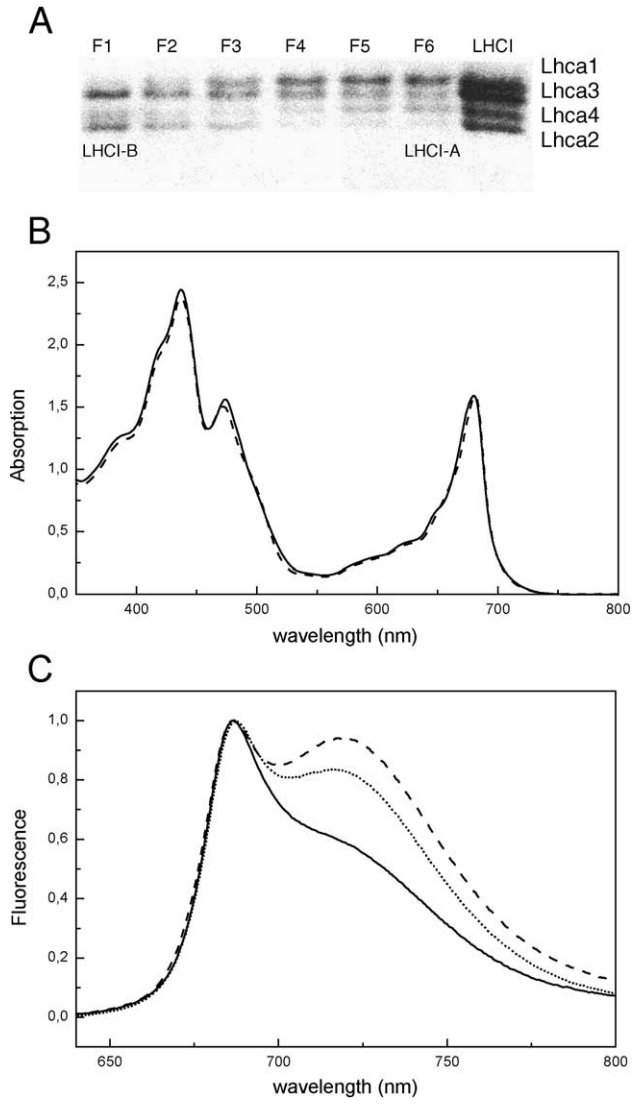

Fig. 3. Analysis of IEF fractions enriched in individual polypeptides. (A) SDS-PAGE of the fractions obtained by IEF on LHCI preparation. The acidity is decreasing from fraction 1 to 6. (B) Absorption spectra at RT of LHCI-A (dashed) and LHCI-B (solid). (C) Fluorescence emission spectra at RT upon excitation at 475 nm of LHCI-A (dashed), LHCI-B (solid) and LHCI fraction before IEF (dotted). All the spectra are normalized to the maximum.

3.2. PSI core to LHCI stoichiometry

We have used SDS-PAGE and densitometry to study the distribution of pigments between PSI core and LHCI. To this end, the Chl concentration of both the PSI–LHCI and LHCI preparation was carefully determined and aliquots were loaded on a SDS-PAGE in four replicates (not shown). After running, gel was stained with Coomassie blue and destained [46]. Densitometry was then performed with the aim of determining the amount of Chl associated with LHCI proteins that had to be loaded in to the gel in order to obtain a level of Coomassie staining of the LHCI associated bands equal to that of the corresponding bands in PSI–LHCI complex. This ratio was 0.43, thus showing that approximately 43% of PSI–LHCI total Chl was associated with LHCI polypeptides. Similar results were obtained using *A. thaliana* and *Z. mays* preparations.

3.3. Reconstituted complexes

The present data clearly indicate that it is not possible to purify the individual Lhca complexes to homogeneity while maintaining the in vivo characteristics. To overcome this problem, Lhca1, Lhca4, and their heterodimeric complex were obtained by in vitro reconstitution using the apoproteins expressed in *E. coli* and reconstituted with pigments and lipids [15]. The reconstituted complexes were purified by sucrose gradient ultracentrifugation and ion exchange chromatography. The reconstitution yield of Lhca4 was lower than for Lhca1, implying a lower stability for this complex. The thermal stability of these pigment–proteins was investigated by the decay of the CD signal at 459 nm with increasing temperature. The denaturation temperature of Lhca1 was 54 °C, while the value dropped to 45 °C for Lhca4, which is the lowest stability of all Lhc complexes so far analyzed [47]. The Lhca1–4 heterodimer is more stable, with a denaturation temperature of 56 °C, similar to the value obtained for the native preparation (57 °C), thus indicating that protein–protein interactions play a role in complex stabilization.

The pigment composition of the three samples was analyzed as reported above. The data are shown in Table 1. Whereas the Chl *a*/*b* ratio in the pigment mix used for reconstitution was the same, the Chl *a*/*b* of refolded Lhca1 was larger than in Lhca4, indicating that Lhca4 has a higher affinity for Chl *b*. The heterodimer has a Chl *a*/*b* ratio intermediate between the two monomers. The Chl/car ratio of the complexes was also very different (3.5 in Lhca1, 5 for Lhca4, and 4.0 for the dimer) as well as the carotenoid composition: β-carotene is not bound to the monomers, while it is bound to the heterodimer.

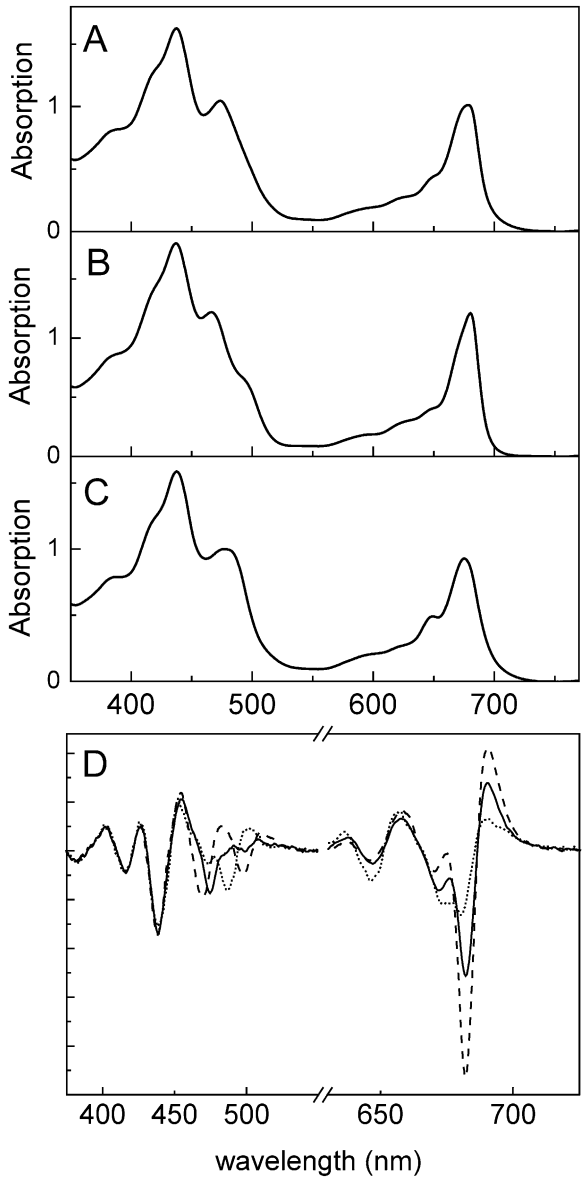

Fig. 4. Absorption spectra at RT of Lhca1–4 dimer (A), Lhca1 (B) and Lhca4 (C). In panel D the second derivatives of the three spectra are reported: Lhca1–4 (solid), Lhca1 (dashed) and Lhca4 (dotted).

The absorption spectra at RT of the complexes are reported in Fig. 4A–C. The absorption maxima of Lhca1, Lhca4, and Lhca1–4 are at 680.5, 675.5 and 679.0 nm, respectively. Absorption tails were also observed at wavelengths longer than 700 nm, particularly in the latter two samples, in agreement with previous measurements [17]. The second derivative analysis of the three spectra is reported in Fig. 4D. In the Q_y region, three main components were observed in all spectra at 646, 672, and 682 nm, although differing in relative amplitude. Major differences were observed in the 480–500-nm interval where the signal can tentatively be associated with the lowest vibrational level of the carotenoid S_2 state. Peaks were detected at 498 and 486 nm for Lhca1 and Lhca4, respectively, while both these components were present in the dimer.

3.4. Linear dichroism (LD) spectra

LD spectra of the three reconstituted samples are shown in Fig. 5. The spectra differ, particularly in the ratio between the amplitude of the Q_y and the Soret signals. In the case of Lhca4, the intensity is almost identical in the two regions, while for both the Lhca1 protein and the Lhca1–4 heterodimer the signal in the red has higher amplitude than that in the blue, similar to the case all PSII antenna complexes[34]. Unfortunately, it is not possible to normalize the LD spectra and thus specifically attribute these features to either a change in carotenoid or Chls orientation. The LD spectra of Lhca1 and Lhca4 peak at 680.0 and 681.5 nm, respectively. In the red absorption tail, a positive contribution is observed in both Lhca4 and Lhca1–4 dimer, indicating that the dipole moment of the Q_y transition forms an angle larger than 54.7° with respect to the normal to the membrane plane. This in agreement with previous measurements on the native preparation [11]. In Lhca1, the red most peak in the Soret region is at 499 nm, while the main signal peaks at 490 nm in Lhca4. In addition, Lhca4 also shows a signal above 500 nm, in agreement with the absorption spectra.

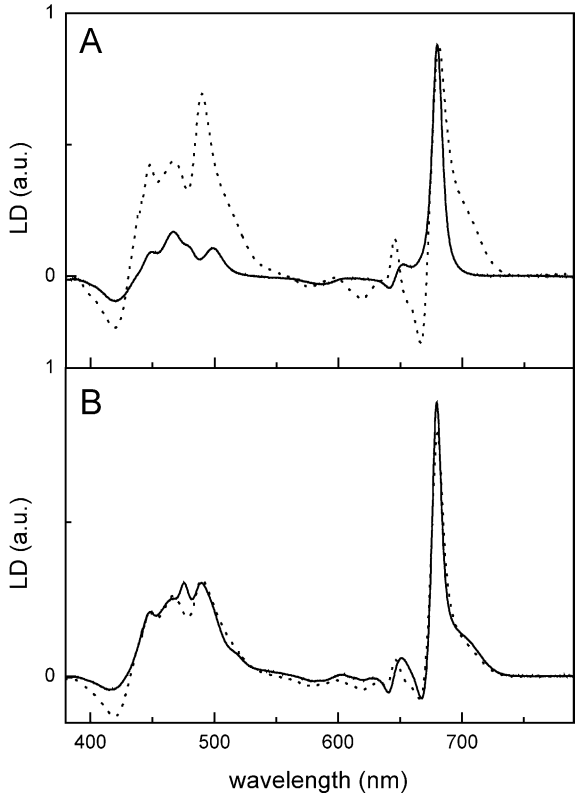

Fig. 5. LD spectra at 100 K. (A) Lhca1 (solid) and Lhca4 (dotted) normalized to the maximum. (B) Lhca1–4 (solid) and sum of Lhca1 and Lhca4 (dotted) normalized as explained in the text (see Results).

In order to analyze the spectral changes that possibly accompany dimerization, we attempted a comparison between the LD spectra of the two monomers with the spectrum of the dimer. To this end, it was necessary to establish the relative contributions of Lhca1 and Lhca4, which was tentatively accomplished by varying their relative ratio and comparing the sum to the spectrum of the heterodimer. The best match was obtained by a 5:7 ratio between the two spectra, as shown in Fig. 5B. The two spectra display similar characteristics in most of the analyzed spectral range. However, there were differences in the 650–660-nm range and in the Soret region where a new signal appears, peaking at 475 nm. These differences can be attributed to Chl *b* molecules on the basis of the peak wavelength, suggesting that Chl *b* chromophores undergo reorganization or coupling to other chromophores upon establishment of monomer–monomer interactions.

3.5. CD spectra

The CD spectra of the three reconstituted samples are presented in Fig. 6. In the Q_y region Lhca1 and Lhca4 are rather different, the former showing three components at 684 (−) nm, 669 (−) nm and 647 (−) nm. Lhca4 shows negative components at 689 (−) nm and 647 (−) nm, where the 647 nm is more intense than in Lhca1. The major difference in this spectral region was the presence of a strong positive signal peaking at 674 nm with a shoulder at approximately 663 nm while the 669 nm (−) was absent. The spectrum of the heterodimer was more similar to Lhca4 than to Lhca1. In the Soret region, the differences are even more pronounced: Lhca4 exhibits strong signal with components at 492 nm (−), 470 nm (−) and 442 nm (+). Lhca1 shows a small, red-shifted signal with respect to the one in the same region of Lhca4 at approximately 504 (−) nm and a more intense negative component at 459 nm.

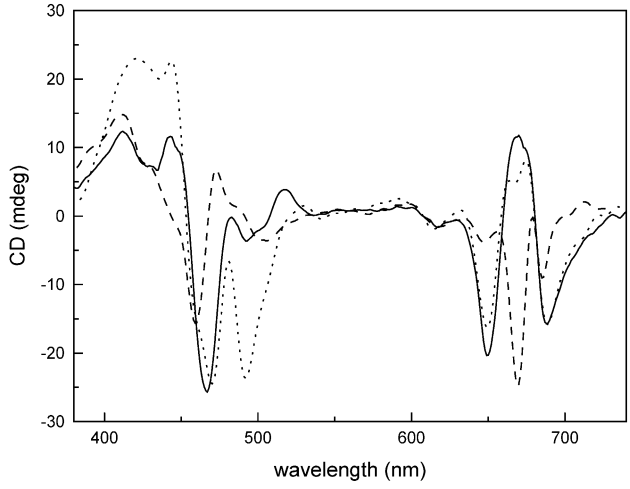

Fig. 6. Circular dichroism spectra at 10 °C of Lhca1–4 (solid), Lhca1 (dashed) and Lhca4 (dotted). The spectra are normalized to the same protein concentration.

The spectrum of the dimer is characterized by an intense signal at 467 nm (−), similar to Lhca4, while the intensity of the 492 nm (−) component is much smaller. From these spectra, it is apparent that dimerization induces conformational changes that are reflected by the chromophore interactions. In particular, the negative contribution at 669 nm of Lhca1 disappears in the dimer, where a positive signal is observed at the same wavelength. This suggests that the Chls, which are responsible for this signal in Lhca1, change their orientation or coupling to other pigments.

In the Soret region, the most interesting feature is associated with the negative 492 nm signal of Lhca4, which disappears almost completely upon dimerization. A similar effect is observed for the positive component at approximately 430 nm. These signals can be tentatively attributed to Chl *a*–carotenoid interaction, which is lost in the dimer, suggesting an environmental change of one carotenoid binding site of Lhca4 upon dimerization.

3.6. Fluorescence spectra

The fluorescence spectra at RT of recombinant Lhca1, Lhca4, and their heterodimeric complex are reported in Fig. 7A. In all cases, the maximum peaks are at 684–686 nm. However, Lhca4 and the Lhca1–4 dimer exhibit a strong shoulder at approximately 720 nm. This red-shifted signal is further displaced to lower energies (732 nm) upon decreasing the temperature 77 K (data not shown) in agreement with previous reports [15]. The excitation energy transfer among chlorophylls was equilibrated as determined by the identical spectral shape obtained upon excitation at different wavelengths, namely 440, 475, and 500 nm (not shown). A minor deviation from this pattern was observed in the Lhca4 complex, consisting in the presence of a new emission at 677 nm upon excitation at 440 nm, and was attributed to a small amount of free Chl *a*. This effect is to be ascribed to the lower stability of this holoprotein rather than to differences in the rate of equilibration between chromophores, as can be judged from its increase in amplitude with the time of incubation.

3.7. Energy transfer efficiency from Car and Chl b to Chl a

The excitation spectra (Fig. 7B) show a major peak at 440 nm and minor contributions from Chl *b* and carotenoids superimposing in a broad shoulder with decreasing amplitude extending to 510 nm. Identical spectra were obtained for both the 685- and 720-nm emission in agreement with the Boltzmann's equilibration of the complexes (see above). Excitation of Lhca1, Lhca4, and Lhca1–4 heterodimer at different wavelengths produced emission spectra with the same shape, implying thermal equilibration among chlorophyll ligands. This result is in contrast to previous reports showing higher contribution by Chl *b* and carotenoids, with respect to Chl *a*, to the red-most emission in both Lhca4 and Lhca1–4 [15]. In the earlier study, this result may have

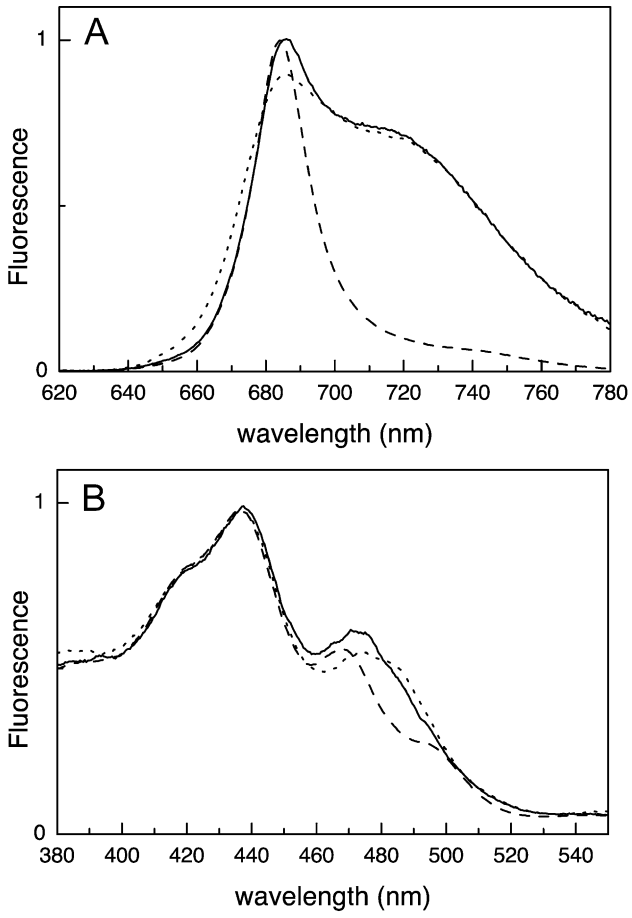

Fig. 7. Fluorescence emission spectra (A) and excitation (B) for Lhca1–4 (solid), Lhca1 (dashed) and Lhca4 (dotted). The spectra are registered at RT and normalized to the maximum. The excitation wavelength was 500 nm for all complexes, while in the excitation spectra the emission was 685 nm for Lhca1 and 720 for Lhca4 and Lhca1–4 complexes.

been due to the presence of uncoupled Chl *a* molecules, which, upon direct excitation at 440 nm, would have led to an artefactual increased amplitude of the Chl *a* emission band.

The spectra were further analysed in order to verify the ability of Chl *b* and carotenoids bound to Lhca proteins in transferring excitation energy to Chl *a*. To this end, the Soret region of the absorption spectra was analysed in terms of the contributions of individual pigments. This was performed by using the deconvolution procedure and the spectral absorption forms of Chl *a*, Chl *b*, and xanthophylls in Lhc protein environment as previously reported [48]. The same description was then used for fitting the fluorescence excitation spectra, and the relative intensity of the individual spectral contributions, after normalisation to 100% transfer efficiency for the Chl *a* contribution, was used to calculate the transfer efficiency from individual pigments [49]. The results show a carotenoid-to-Chl transfer efficiency very close to 65% in the three samples. This figure is lower than in Lhcb proteins for which a value close to 75% were previously reported by using the same procedure [47].

4. Discussion

4.1. Pigment-to-protein stoichiometry

Analysis of pigment-to-protein stoichiometry on the native LHCI fraction (which contains all four Lhca complexes) yields 10 ± 0.5 bound Chls and around 2.3 carotenoids per polypeptide in both *Z. mays* and *A. thaliana* [9].

Lhcb proteins bind either three (LHCII, [45]) or two (CP29, CP26, CP24, [44]) xanthophylls per polypeptide while strong homology suggests a similar figure for Lhca proteins. The Chl-to-Car ratio of Lhca1 and Lhca4 was 3.35 and 4.90, respectively. These values are consistent with Lhca1 and Lhca4 binding 10 Chls each plus three and two xanthophylls per polypeptide, respectively. Different figures would yield non-integer values for the number of xanthophyll binding sites in contrast with previous determinations in recombinant Lhc proteins. This is consistent with the report of 10 Chl per polypeptide in CP24, the only Lhcb protein clustering with Lhca in sequence analysis [50]. A value as low as 5 was previously suggested for the number of Chls bound to Lhca1 and Lhca4 [15]. However, the value of 5 Chls per polypeptide would be inconsistent with the conservation of 8 Chl binding residues [50], which have been experimentally shown to bind Chls in both LHCII and CP29 [44,45]. Our stoichiometric determinations of 10 Chls per polypeptide in nLHCI would imply 15 Chls per polypeptide for both Lhca2 and Lhca3, which seems improbable. Based on the above considerations and on stoichiometry of 2.3 cars per 10 Chl in the native complex containing the four Lhca polypeptides, we conclude that only one of the four Lhca proteins, i.e. Lhca1, binds three xanthophylls. Lhca4, -2, and -3 bind two xanthophyll molecules per polypeptide each while all of them bind 10 Chls. Small deviations from these values cannot be excluded for Lhca3 and Lhca2 but seem unlikely due to the strong homology with CP24 [51].

4.2. PSI core to Lhca stoichiometry

Densitometric analysis of SDS-PAGE gels loaded with PSI–LHCI and LHCI preparations showed that 43% of total Chl was associated with LHCI. Since the number of Chls associated with PSI core in barley was determined to be 111 ± 4 [2] the total number of Chls in the PSI–LHCI complex can be calculated as 195 ± 6 and the LHCI moiety should bind 84 ± 3 Chls. Since we have determined a value of 10 Chls per LHCI polypeptide, it follows that there are approximately 8 Lhca polypeptides per PSI core complex.

4.3. Lhca4

The recombinant Lhca4 complex is the least stable of all the Lhc proteins, its melting temperature being at 45 °C, well below that of Lhca1 (54 °C) and of the other Lhc proteins (64–77 °C). It should be noted, however, that the Lhca1/Lhca4 has essentially the same melting temperature

as that of Lhca1 (56 vs. 54 °C), thus suggesting that upon dimerization Lhca4 assumes a more stable conformation. The Lhca4 complex binds 7 Chl *a*, 3 Chl *b*, and 2 carotenoid molecules: 0.5 violaxanthin and 1.5 luteins. This xanthophyll complement is similar to what was observed for the two central sites, L1 and L2, of LHCII complex. By analogy with other Lhc proteins binding two xanthophylls per polypeptide, i.e. CP29, CP26, and CP24, we suggest that the xanthophyll binding sites conserved in Lhca4 correspond to L1 and L2 sites of LHCII. The absorption spectrum of Lhca4 is characterized by a red absorption tail at wavelengths longer than 700 nm. This band is featureless even at low temperature (not shown), indicating a very large FWHM. The fluorescence emission at RT shows a maximum at 686 nm and a shoulder at 720 nm, which originates from the red absorption in agreement with previous results [23,11]. At low temperature the maximum is red-shifted to 732 nm as shown in previous reports [15] (data not shown). The LD spectrum is quite peculiar when compared to the LD spectra of all other antenna complexes, not only for the presence of a positive contribution associated with the red forms, but also because the amplitude of the spectrum in the Q_y range is similar to that in the Soret region. A more quantitative evaluation is possible upon normalization of Lhca4 and Lhca1 spectra (Fig. 5A) based on fitting the dimer LD spectrum to obtain a spectral sum similar to the dimer (Fig. 5B). Whereas we need to be cautious about this normalization procedure, the good match between the two spectra in Fig. 5B suggests the 5:7 ratio between the amplitude of Lhca4 and Lhca1, respectively, is reasonable. The comparison shows marked differences in the intensity of the LD signal in the carotenoid absorption region (430–520 nm). This suggests that at least one xanthophyll in Lhca4 is differently oriented and its transition moment, lying close to the polyene chain [52], forms a larger angle with the normal to the membrane plane. The main signal in Q_y region is associated with a Chl *a* form absorbing at 681.5 nm, while the signal is very low around 675 nm, at the maximum of the absorption. This suggests that the positive LD spectrum of this complex is mostly associated with a Chl *a* absorbing at 681 nm. A similar behavior was observed in LHCII, where the LD positive signal was attributed to the Chl *a* in site A2 also absorbing at 681 nm[34].

4.4. Lhca1

The Lhca1 complex binds Chl *a* and Chl *b* with a ratio of 4.0 and the total Chl (*a*+*b*) to Car is 3.35 corresponding to a Chl complement of 8 Chl *a*, 2 Chl *b*. Moreover, 2 luteins and 1 violaxanthin per polypeptide are probably located in sites L1, L2, and N1 in agreement with previous results with Lhc proteins [10,53,54]. Lhca1 shows higher reconstitution yield and stability as compared to Lhca4.

The Q_y absorption peak of Lhca1 is localized at 680.5 nm at RT while the fluorescence emission is located at 684 nm and a contribution at 701 nm is also visible at LT, indication of the presence of low energy forms [15]. While it is well established that Lhca4 contains red-shifted Chl *a* absorption forms [15], it was previously reported that Lhca1 has none. This does not seems to be completely true: in fact, contributions at wavelengths as long as 690 nm and low amplitude contributions at 700 nm are also apparent. Further support to the presence of low energy absorption forms is provided by the comparison with the fluorescence emission spectra of recombinant Lhca1 reconstituted with Chl *a* only (Fig. 8). A detailed analysis of this pigment–protein complex is outside the scope of this manuscript and will be presented in a forthcoming paper; however, it is clear that the red side broadening of the Lhca1 spectrum depends on the presence of Chl *b*. Similar results have been shown for Lhca4 [55] in which the intense red-shifted (732 nm) emission peak was completely abolished by the lack of Chl *b*. These results both confirm the presence of low energy absorption forms in Lhca1 and strongly suggest they originate from the same protein domains as the 720-nm emission peak of Lhca4.

To investigate the distribution of Chl electronic transitions in Lhca1, the absorption spectrum in the Q_y transition was fitted with the spectra of Chl *a* and Chl *b* in protein environment (Fig. 9, as in Ref. [34]). Two Chl *b* forms and six Chl *a* forms were needed in order to fit the spectrum. The two Chl *b* show maxima at 644 and 652 nm, each accounting in amplitude for one Chl. The six Chl *a* forms peak at 663, 669, 676, 682.4, 689, and 700 nm, respectively. The 689-nm form accounts for 0.75 Chl *a* molecule, while the intensity of the 700-nm form represents only 1% of the absorption. It is reasonable to suppose that these are the absorption forms responsible for the emission contribution at 702 nm. While the low energy absorption forms of Lhca1 are less red-shifted than in Lhca4, it is clear that

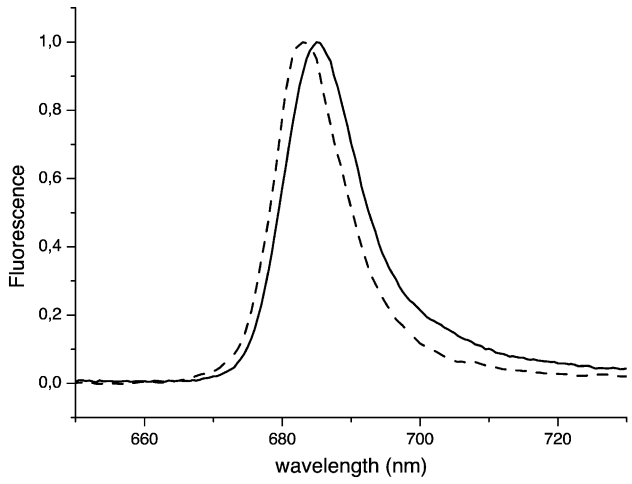

Fig. 8. Comparison of the emission spectra at 77 K of Lhca1 (solid) and Lhca1–Chl *a* (dashed) excited at 475 nm. The spectra are normalized to the maximum.

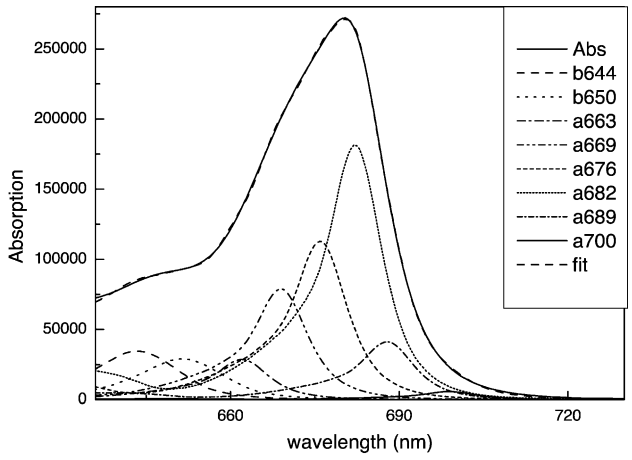

Fig. 9. Fitting of the absorption spectrum of Lhca1 at RT with the spectra of Chl *a* and Chl *b* in protein environment [34].

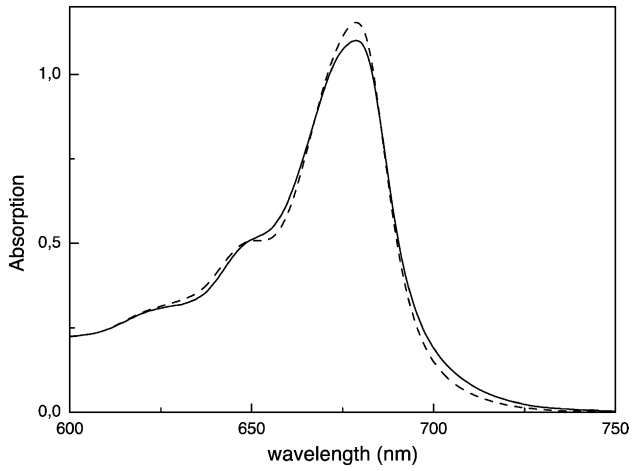

Fig. 10. Comparison of the absorption spectra of Lhca1–4 dimer (solid) with the sum of the spectra of (Lhca1 and Lhca4)/2 (dashed). The spectra are normalized to the protein concentration.

the protein scaffold is modulating the spectroscopic characteristics of the individual Chls in Lhca1 differently compared to PSII antenna system, shifting most of the Chl transitions to lower energy. In fact, the amplitude of the 682.4-nm form in Lhca1 accounts for three Chl *a* molecules while in LHCII, CP29, and CP26, the red-most Chl *a* form, absorbing at 681 nm, was associated with only one Chl located in site A2 [44,45]. The red-shift effect on Lhca1 chromophores also extends to at least one xanthophyll molecule, whose red-most peak was at 499 nm (Fig. 4D), 4–7 nm with respect to the absorption of violaxanthin or lutein in LHCII [54].

4.5. Lhca1–Lhca4 dimer

Lhca1 and Lhca4 assemble in vitro to form heterodimers according to a previous report [15]. The biochemical properties of the dimer are intermediate between the two monomers. In addition, the dimer bound small amounts of β-carotene, which is not present in the monomers. Since there is no increase of xanthophyll content in the dimer with respect to the sum of monomers, we suggest that folding in the presence of the partner protein changes the affinity of one carotenoid binding site which can now accommodate β-carotene.

Several lines of evidence indicate that dimerization affects the chromophore organization: CD and fluorescence spectra of the dimer are different as compared to the sum of the monomers, and the LD analysis indicates a change in the orientation of Chl *b* as compared to the sum of monomers. In order to investigate if the dimerization process also affects the red-shifted absorption, we compared the spectrum of the dimer with the sum of the spectra of Lhca1 and Lhca4 upon normalization to the protein content. The result is presented in Fig. 10. The two spectra are quite similar but an increase by 30% is observed in the amplitude of the red tail. This is compensated by a decreased absorption at 678 nm. This suggests that the protein–protein interactions play a role in the red absorption similar to the case of the bacterial reaction center [56].

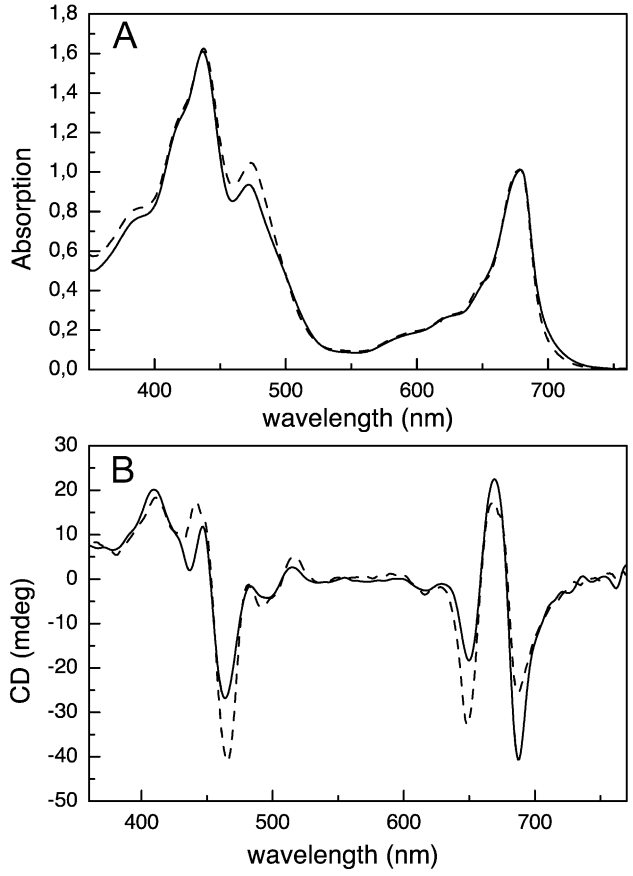

Fig. 11. Comparison between the spectroscopic characteristics of the LHCI native fraction (solid) and Lhca1–4 reconstituted dimer (dashed). (A) Absorption spectra at RT normalized to the maximum; (B) CD spectra at 10 °C normalized to the absorption.

4.6. Lhca2 and Lhca3

In most of the reports present in the literature, purification of LHCI complexes by sucrose gradient ultracentrifugation yielded two bands: the upper was named LHCI-680 from the peak in fluorescence emission spectrum and contained Lhca2 + Lhca3. The lower band (LHCI-730) contained Lhca1 + Lhca4 [3]. On this basis it was argued that Lhca2 and Lhca3 do not contain "red" Chls. However, spectroscopic analysis of the LHCI preparation [11] and anti-sense experiments, where the absence of Lhca2 or Lhca3 was correlated to a blue shift of the red fluorescence peak [22], suggested "red" Chls might be associated to Lhca2 and Lhca3. The LHCI-680 fraction was not present in our experiments, suggesting that mild procedures were effective in maintaining all Lhca polypeptides in their dimeric form. A monomeric LHCI band showing a 690-nm emission was only obtained upon harsh treatment of the LHCI fraction with detergent (data not shown). The analysis of this fraction, which was indeed enriched in Lhca3 and Lhca2 polypeptides, reveals that these complexes were present in monomeric form and were showing a lower Chl *a*/*b* ratio [9]. We conclude that the LHCI-680 (or 690) fraction is the product of artefactual monomerization while native Lhca2 and -3 are, in fact, dimers. Whereas it was not possible to purify to homogeneity Lhca2 and Lhca3 in dimeric state, fractions enriched in these two complexes were obtained. The Lhca2/3-enriched fraction showed a red tail in the absorption spectra, whose amplitude was similar to that of fractions enriched in Lhca1–4. This was associated to red-shifted fluorescence emission. An additional evidence for the association of "red" absorption and emission forms to Lhca2 and Lhca3 is obtained by comparing absorption and fluorescence emission spectra of the recombinant Lhca1–4 heterodimeric complex with the native LHCI preparation: they have similar amplitude of "red" forms in both fluorescence and absorption spectra (Fig. 11A), thus implying that Lhca2/3 dimers have similar content in red forms as Lhca1–4. The two types of dimers are likely to have similar pigment organization as indicated (Fig. 11) by the very similar absorption and CD spectra of the native LHCI and the recombinant heterodimer.

Acknowledgements

This work was founded by CNR "agenzia 2000" and by "MIUR" Progetto FIRBn.RBAU01ECX.

References

[1] P. Jordan, P. Fromme, H.T. Witt, O. Klukas, W. Saenger, N. Krauss, Nature 411 (21-6-2001) 909–917.
[2] J. Knoetzel, A. Mant, A. Haldrup, P.E. Jensen, H.V. Scheller, FEBS Lett. 510 (16-1-2002) 145–148.
[3] R. Bassi, D. Simpson, Eur. J. Biochem. 163 (1987) 221–230.
[4] S. Jansson, Biochim. Biophys. Acta 1184 (1994) 1–19.
[5] E.J. Boekema, P.E. Jensen, E. Schlodder, J.F. van Breemen, H. van Roon, H.V. Scheller, J.P. Dekker, Biochemistry 40 (2001) 1029–1036.
[6] P.E. Jensen, M. Gilpin, J. Knoetzel, H.V. Scheller, J. Biol. Chem. 275 (2000) 24701–24708.
[7] H.V. Scheller, P.E. Jensen, A. Haldrup, C. Lunde, J. Knoetzel, Biochim. Biophys. Acta 1507 (2001) 41–60.
[8] I. Damm, D. Steinmetz, L.H. Grimme, in: M. Baltscheffsky (Ed.), Current Research in Photosynthesis, vol. II, 1989, pp. 607–610.
[9] R. Croce, R. Bassi, in: G. Garab (Ed.), Photosynthesis. Mechenisms and Effects, vol. I, 1998, pp. 421–424.
[10] W. Kühlbrandt, D.N. Wang, Y. Fujiyoshi, Nature 367 (1994) 614–621.
[11] J.A. Ihalainen, B. Gobets, K. Sznee, M. Brazzoli, R. Croce, R. Bassi, R. van Grondelle, J.E.I. Korppi-Tommola, J.P. Dekker, Biochemistry 39 (2000) 8625–8631.
[12] B. Gobets, J.T.M. Kennis, M. Brazzoli, R. Croce, I.H. van Stokkum, R. Bassi, J.P. Dekker, H. Van Amerongen, G.R. Fleming, R. van Grondelle, J. Phys. Chem., B 105 (2001) 10132–10139.
[13] J. Knoetzel, I. Svendsen, D.J. Simpson, Eur. J. Biochem. 206 (1992) 209–215.
[14] S.E. Tjus, M. Roobol-Boza, L.-O. Palsson, B. Andersson, Photosynth. Res. 45 (1995) 41–49.
[15] V.H.R. Schmid, K.V. Cammarata, B.U. Bruns, G.W. Schmidt, Proc. Natl. Acad. Sci. U. S. A. 94 (1997) 7667–7672.
[16] A.N. Melkozernov, S. Lin, V.H.R. Schmid, H. Paulsen, G.W. Schmidt, R.E. Blankenship, FEBS Lett. 471 (2000) 89–92.
[17] A.N. Melkozernov, V.H.R. Schmid, G.W. Schmidt, R.E. Blankenship, J. Phys. Chem., B 102 (1998) 8183–8189.
[18] R. Croce, G. Zucchelli, F.M. Garlaschi, R. Bassi, R.C. Jennings, Biochemistry 35 (1996) 8572–8579.
[19] B. Gobets, R. van Grondelle, Biochim. Biophys. Acta 1057 (2001) 80–99.
[20] H. Zhang, H.M. Goodman, S. Jansson, Plant Physiol. 115 (1997) 1525–1531.
[21] J. Knoetzel, B. Bossmann, L.H. Grimme, FEBS Lett. 436 (1998) 339–342.
[22] U. Ganeteg, A. Strand, P. Gustafsson, S. Jansson, Plant Physiol. 127 (2001) 150–158.
[23] R. Croce, G. Zucchelli, F.M. Garlaschi, R.C. Jennings, Biochemistry 37 (1998) 17255–17360.
[24] R. Bassi, U. Hinz, R. Barbato, Carlsberg Res. Commun. 50 (1985) 347–367.
[25] U.K. Laemmli, Nature 227 (1970) 680–685.
[26] P. Dainese, G. Hoyer-hansen, R. Bassi, Photochem. Photobiol. 51 (1990) 693–703.
[27] J. Sambrook, E.F. Fritsch, T. Maniatis, Molecular Cloning. A Laboratory Manual, 2nd ed., Cold Spring Harbor Laboratory Press, USA, 1989.
[28] T.J. Gibson (1984). Thèsis.
[29] S. Gottesman, E. Halpern, P. Trisler, J. Bacteriol. 148 (1981) 263–265.
[30] K. Nagai, H.C. Thøgersen, Methods Enzymol. 153 (1987) 461–481.
[31] H. Paulsen, S. Hobe, Eur. J. Biochem. 205 (1992) 71–76.
[32] E. Giuffra, D. Cugini, R. Croce, R. Bassi, Eur. J. Biochem. 238 (1996) 112–120.
[33] A.M. Gilmore, H.Y. Yamamoto, Plant Physiol. 96 (1991) 635–643.
[34] R. Croce, G. Canino, F. Ros, R. Bassi, Biochemistry 41 (2002) 7334–7343.
[35] C.H.W. Hirs, Methods Enzymol. 11 (1967) 325–329.
[36] A. Pagano, G. Cinque, R. Bassi, J. Biol. Chem. 273 (1998) 17154–17165.
[37] P. Haworth, C.J. Arntzen, P. Tapie, J. Breton, Biochim. Biophys. Acta 679 (1982) 428–435.
[38] P. Haworth, P. Tapie, C.J. Arntzen, J. Breton, Biochim. Biophys. Acta 682 (1982) 152–159.

[39] E. Giuffra, G. Zucchelli, D. Sandona, R. Croce, D. Cugini, F.M. Garlaschi, R. Bassi, R.C. Jennings, Biochemistry 36 (1997) 12984–12993.
[40] G. Cinque, R. Croce, R. Bassi, Photosynth. Res. 64 (2000) 233–242.
[41] E.J. Boekema, H. van Roon, F. Calkoen, R. Bassi, J.P. Dekker, Biochemistry 38 (1999) 2233–2239.
[42] R. Harrer, R. Bassi, M.G. Testi, C. Schäfer, Eur. J. Biochem. 255 (1998) 196–205.
[43] P. Dainese, R. Bassi, J. Biol. Chem. 266 (1991) 8136–8142.
[44] R. Bassi, R. Croce, D. Cugini, D. Sandona, Proc. Natl. Acad. Sci. U. S. A. 96 (1999) 10056–10061.
[45] R. Remelli, C. Varotto, D. Sandona, R. Croce, R. Bassi, J. Biol. Chem. 274 (1999) 33510–33521.
[46] E.H. Ball, Anal. Biochem. 155 (1986) 23–27.
[47] E. Formaggio, G. Cinque, R. Bassi, J. Mol. Biol. 314 (2001) 1157–1166.
[48] R. Croce, G. Cinque, A.R. Holzwarth, R. Bassi, Photosynth. Res. 64 (2000) 221–231.
[49] R. Croce, M.G. Muller, R. Bassi, A.R. Holzwarth, Biophys. J. 80 (2001) 901.
[50] E. Pichersky, S. Jansson, in: D.R. Ort, C.F. Yocum (Eds.), Oxygenic Photosynthesis: The Light Reactions. Dordrecht 1996, pp. 507–521.
[51] R. Bassi, E. Giuffra, R. Croce, P. Dainese, E. Bergantino, in: R.C. Jennings, G. Zucchelli, F. Ghetti, G. Colombetti (Eds.), Light as an Energy Source and Information Carrier in Plant Physiology NATO ASI Series. Series A: Life Sciences, vol. 287, Plenum, New York, 1996, pp. 41–63.
[52] P.M. Dolan, D. Miller, R.J. Cogdell, R.R. Birge, H.A. Frank, J. Phys. Chem., B 105 (2001) 12134–12142.
[53] R. Croce, R. Remelli, C. Varotto, J. Breton, R. Bassi, FEBS Lett. 456 (1999) 1–6.
[54] R. Croce, S. Weiss, R. Bassi, J. Biol. Chem. 274 (1999) 29613–29623.
[55] V.H.R. Schmid, P. Thome, W. Ruhle, M.D. Paulsen, W. Kuhlbrandt, H. Rogl, FEBS Lett. 499 (2001) 27–31.
[56] N.V. Karapetyan, D. Dorra, A.R. Holzwarth, J. Kruip, M. Rögner, in: G. Garab (Ed.), Photosynthesis: Mechanisms and Effects, vol. I, 1998, pp. 583–586.